J Mater Sci (2010) 45:5109–5117
DOI 10.1007/s10853-010-4472-x

ICAM 2009

Mechanical testing of cordierite porous ceramics using high temperature diametral compression

M. L. Sandoval · M. H. Talou · A. G. Tomba Martinez · M. A. Camerucci

Received: 29 October 2009 / Accepted: 5 April 2010 / Published online: 23 April 2010

Abstract In this study, the high temperature mechanical behavior of cordierite porous disks prepared by the starch consolidation forming method was evaluated. In this method, due to the swelling and gelatinization properties of starch in aqueous suspension at a temperature between 55 and 85 °C, the starch granules perform as both consolidator/binder of the green body and pore former at high temperature. Aqueous suspensions (29.6 vol.%) of a cordierite precursor mixture (talc, kaolin, and alumina) with the addition of potato or cassava starches (11.5 vol.%) were prepared by intensive mechanical mixing, homogenization, and vacuum degasification. Green disks were formed by thermogelling of the aqueous suspensions at 85 °C for 4 h followed by additional drying at 50 °C for 24 h. They were characterized by bulk density and apparent porosity measurements, and microstructural analysis by scanning electron microscopy (SEM) and energy dispersive X-ray spectroscopy (EDS). Porous cordierite materials were obtained by calcination at 650 °C for 2 h and reaction-sintering at 1330 °C for 4 h, employing specific, controlled heating schedules in both treatments. Cordierite disks were characterized by bulk density and apparent porosity measurements, and microstructural analysis by SEM. Mechanical behavior was evaluated in diametral compression using a servohydraulic testing machine at room temperature (*RT*), 800, 1000, and 1100 °C. Apparent stress–strain relationships were obtained from load–displacement curves, and mechanical parameters, such as fracture strength (σ_F), apparent Young modulus (E_a), and yield stress (σ_Y), were determined. Moreover, crack patterns were also evaluated. The obtained results were analyzed in function of the developed microstructures, considering the presence of a silicate glassy phase and a complex porosity, and the testing temperature.

M. L. Sandoval · M. H. Talou · A. G. Tomba Martinez (✉) · M. A. Camerucci
Laboratorio de Materiales Estructurales, División Cerámicos, INTEMA, Av. Juan B. Justo 4302, Mar del Plata 7600, Argentina
e-mail: agtomba@fi.mdp.edu.ar

Introduction

Porous ceramic materials require the development of specific homogenously distributed porosity, pore size distribution, and pore morphology, to be suitable for each one of their many applications. The potential uses of these materials cover a wide range of technological applications, such as catalyst supports, filters, combustion burners, and thermal insulators, among others [1, 2]. In the past few years, several new processing methods have been developed to satisfy the high demand of materials with controlled porous microstructures [1–3].

Among the forming methods by direct consolidation, in which the ceramic suspension consolidates in non-porous moulds (e.g., metal molds) without compaction or removal of water, a new non-contaminating low-cost technique, based on the gelling capability of starch in aqueous media at a temperature range (55–85 °C), has been developed for use in the manufacture of porous ceramics. The starch acts as both a consolidator/binder agent of the ceramic particles and a pore former after consolidation by burn-out at high temperature [4–6]. During the gelatinization process, starch granules undergo a rapid and irreversible swelling by water absorption [7], causing the ceramic particles to stick together and, consequently, consolidate into a solid body.

This method has been successfully employed for the production of porous bodies of alumina [8, 9], cordierite [4], and mullite [10], among others.

Cordierite ($2Al_2O_3{\cdot}5SiO_2{\cdot}2MgO$) is a potential material to be used as thermal insulators, among others applications, because of its low thermal expansion coefficient ($\alpha = 1–3 \times 10^{-6°C-1}$) and thermal conductivity (1–2 W/mK) [11]. In addition, particularly for this and some other applications, the development of porous ceramics with good mechanical response even at high temperature is necessary. However, the mechanical evaluation of these pieces is more frequently accomplished only at room temperature (*RT*).

Furthermore, the application of porous ceramics as structural components at high temperature requires the evaluation of the mechanical properties in conditions similar to those in which they are used. However, these data are scarce in the literature, particularly for cordierite materials.

On the other hand, the diametral compression test has been usually employed in the mechanical evaluation of green compacts [12, 13] due to its several advantages: simpler specimen preparation, simple geometry, quickness of testing, independent data with regard to surface finish, and the absence of edge effects. This test has also been used, although less frequently, to test sintered bodies [14–16]. However, the use of diametral compression test for high temperature evaluation is very uncommon.

The aim of this study is to evaluate the high temperature mechanical behavior of cordierite-based porous bodies prepared by thermogelling of aqueous ceramic suspensions with potato or casava starches, using the diametral compression test. The mechanical response of both materials as a function of the temperature was analyzed taking into account the presence of a glassy phase, together with the different porosities generated by the burning of starch at high temperature.

Experimental

Raw materials and characterization

A mixture of commercially available powders of kaolin (kaolin C-80, Stone Big CORP., Arg.), talc (Talc 40, China), and alumina (A2G Alcoa, USA), with particle sizes <5 μm, was used as a cordierite precursor. The mineralogical qualitative analysis of the as-received powders was carried out by X ray-diffraction (XRD; Philips PW3710, Cu Kα radiation, at 20 mA and 40 kW). In the kaolin powder, kaolinite ($Al_2Si_2O_5(OH)_4$, File 06-0221) was determined to be the main crystalline phase, together with vestiges of quartz (SiO_2, File 5-0490) and orthoclase ($KAlSi_3O_8$, File 31-0966). Talc ($Mg_3Si_4O_{10}(OH)_2$, File 19-0770) was the main crystalline phase in the mineral of talc, together with vestiges of dolomite ($CaMg(CO_3)_2$, File 34-0517) and magnesite ($MgCO_3$, File 83-1461). Corundum (α-Al_2O_3, File 42-1468) was the only identified phase in the alumina powder. The cordierite precursor mixture was formulated with 37 wt% of kaolin, 41 wt% of talc, and 22 wt% of alumina, which gives a composition with less silica content than that of the stoichiometric cordierite (SiO_2 = 51.4 wt%; Al_2O_3 = 34.8 wt% and MgO = 13.8 wt%). According to the global composition, 85.7 wt% of cordierite and 14.3 wt% of $Al_2O_3{\cdot}MgO$ spinel were estimated as being the final phases in thermodynamic equilibrium.

Native potato and cassava starches commercially available in Argentina were used as a consolidator/binder and a pore former agent. Real densities determined using helium pycnometry (Quanta-Chrome, USA) were 1.47 and 1.49 g/cm^3 for potato and cassava starches, respectively. The particle size distributions (Malvern Instruments Ltd, UK) were determined using an aqueous suspension of starch with a polyacrylic acid (Dolapix CE-64, Zschimmer & Schwarz, Germany) as a dispersant, and applying ultrasound for 15 min to disperse and stabilize the starch particles. Both starches presented bimodal distributions, with a low percentage volume of small granules that can be associated with impurities or broken granules. The mean particle diameter for potato starch (D_{50} = 47.8 μm) was notably higher than that of cassava starch (D_{50} = 13.6 μm). The latter showed a higher amount of small granules (0.5–3 μm) than potato starch (1–10 μm). The parameter $W = D_{90} - D_{10}/D_{50}$ (where D_{90} and D_{10} are the granule diameters for 90 and 10 vol.% of granules, respectively) was chosen for estimating the width of particle size distributions. Both starches presented a relatively wide distribution with *W* values of 1.3 and 1.2 for potato and cassava starches, respectively. The weight percentage of humidity was determined by means of thermogravimetric analysis (Shimatzu, TGA-50) at a heating rate of 10 °C/min up to 120 °C, in air, and the following values were obtained: 14.4 wt% for potato starch and 11.5 wt% for cassava starch. The granular morphology analysis of the dry starches was carried out by scanning electron microscopy (Jeol JSM-6460). Potato starch exhibited the larger granules, with smooth surfaces and oval or spherical forms while cassava starch exhibited granules with some polyhedral morphology [17].

By means of pycnometry in kerosene at 37 °C, the pycnometric density (δ^{p}_{pic}) value for the precursor mixture was determined to be 2.44 ± 0.06 g/cm^3.

Preparation and characterization of green bodies

Green disks (diameter = 15.0 mm; thickness = 4.2–2.3 mm) were prepared by thermogelling of aqueous suspensions of the

cordierite precursor mixture (29.6 vol.%) and 11.5 vol.% of each starch. This starch content is usually used to produce porous ceramics with porosities >35 vol.% in the starch consolidation technique [5]. The suspensions were prepared by (a) mixing (impeller mixer) ceramic powders in water (70.4 vol.%) with 1 wt% of Dolapix CE-64 (Zschimmer & Schwarz, Germany) and 0.5 wt% of sodium naphtalenesulfonate (both with respect to the content of ceramic solids), added in a sequential manner (kaolin first, followed by a wait of 24 h, then the talc, and finally the alumina); (b) homogenization in a ball mill, 2 h; (c) addition of starch and mixing (impeller mixer) for 3 min; and (d) degassing for 20 min. The suspensions were poured into cylindrical stainless steel molds (which were covered with Teflon tape to reduce water evaporation), heated in air at 85 °C for 4 h (Memmert, universal oven with forced air circulation) and dried at 50 °C for 12 h. The disks were machined using 600-grit SiC paper to obtain flat and parallel surfaces.

The average green densities (δ_v) were determined by immersion in Hg (Archimedes method) and the disk porosities ($\%P_v$) were calculated as $100 \times (1 - \delta_v/\delta_{pic}^p)$. The values of δ_v- $\%P_v$ were 1.20 ± 0.04 g/cm^3- $51 \pm 2\%$ and 1.30 ± 0.05 g/cm^2- $47 \pm 2\%$ for disks prepared with potato and cassava starches, respectively.

The microstructural analysis of the green disks obtained by the thermogelling of potato or cassava starches was carried out by SEM (Jeol JSM-6460) and EDS (EDAX-Genesis XM-2-Sys). Micrographs of the green compacts are presented in Fig. 1. When starch granules are heated in the presence of water, several changes such as water diffusion, granule swelling, amylose leaching, disruption of crystalline structures, and realignment and formation of new intermolecular and intramolecular bonds occur in a process called 'gelatinization' [18]. Swollen starch granules and original granules that did not swell together with leached components from gelatinized granules form a three-dimensional (3D) gel network. In both images, swelled and non-swelled starch granules (marked with arrows) are shown. These observations were confirmed by elementary analysis of carbon (EDAX, Fig. 1). The sizes and morphologies of the granules observed by SEM were within the range of the values determined for dry and gelatinized starches [18, 19].

Preparation and characterization of cordierite porous disks

After drying, green disks were calcinated at a heating rate of 1 °C/min up to 650 °C for 2 h. Porous cordierite materials were produced by reaction-sintering using a controlled thermal cycling up to 1330 °C, 4 h (heating at 3 °C/min and cooling at 5 °C/min to *RT*) [16]. An electrical furnace (Carbolite) with SiC heater elements was used for both treatments.

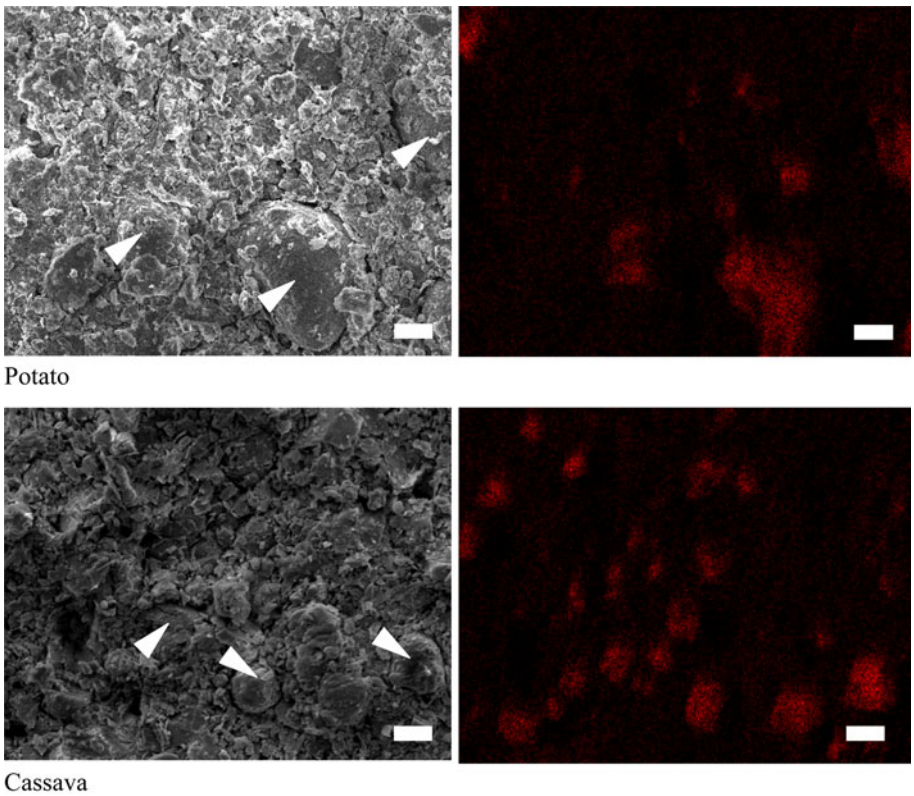

Fig. 1 SEM/EDAX micrographs of green bodies (*arrows* show some starch granules) and carbon mapping (bars = 10 μm)

Disks 13.0–14.0 mm in diameter and 2.8–3.0 mm in thickness were obtained. The labels for the porous disks were P and C for disks prepared with potato and cassava starches, respectively.

Sintered porous bodies were characterized by XRD (Philips, Cu Kα radiation, at 30 mA and 40 kW) employing powdered samples. In both materials, P and C, cordierite was determined as the main crystalline phase ($Mg_2Al_4Si_5O_{18}$, File 13-293) together with $Al_2O_3{\cdot}MgO$ spinel (File 5-0672) and a very small amount of alumina as corundum (α-Al_2O_3, File 42-1468). None of the peaks characteristic of raw materials were identified. It was also observed that the baseline rose in the range 20–30°2θ, which corresponds to the region of maximum diffraction peaks of silicate crystalline phases. Based on this fact, the presence of a silicate glassy phase that came from impurities of raw materials and the decomposition of kaolinite was inferred. In both cases, low melting point silicates were generated, which reduced the temperature for liquid formation of the $SiO_2{\cdot}Al_2O_3{\cdot}MgO$ ternary system (1350 ± 5 °C) [20].

The bulk density of sintered disks (δ_s) was measured by immersion in Hg (Archimedes method) and the porosities ($\%P_s$) were calculated as $100\times(1-\delta_v/\delta^s_{pic})$ using the pycnometric density of the powder obtained at 1330 °C, 4 h [16]: ($\delta^s_{pic} = 2.69$ g/cm^3 ± 0.04). The values of δ_s- $\%P_s$ were 1.20 ± 0.04 g/cm^3- 55 ± 2% and 1.42 ± 0.04 g/cm^3- 47 ± 2% for P and C disks, respectively. The porosity was higher for disks obtained by using potato starch, following the same tendency of green bodies. After sintering, all the disks exhibited porosity levels rather higher than the original starch content (11.5%) and a volumetric shrinkage of ~9%. These results could be attributed to the swelling of numerous granules during the consolidation process, and the occurrence of densification in the ceramic matrix due to a liquid phase-assisted sintering mechanism [19] during high-temperature treatment. Thus, the porosity present in the sintered bodies was associated with both, large pores originated by burning of original, swelled, or adjacent starch granules and small pores coming from the incomplete densification of the ceramic matrix (Fig. 2).

Microstructural analysis was performed by SEM (Jeol JSM 6460) on surfaces polished with diamond pastes of 6, 3, and 1 μm. Before polishing, the samples were impregnated with epoxy resin in vacuum. SEM images of porous P and C disks are displayed in Fig. 2. The size and morphology of the pores were determined by means of analyzing the SEM micrographs with image analysis software (Image-Pro Plus, Media Cybernetics). The equivalent circular diameter calculated as the average of the values of diameters that pass through the center of each individual pore measured with a step of 2° was selected as a parameter to quantify pore size. However, a deeper analysis is needed to characterize the complex features of the porosity generated by starch removal; this is the objective of other research currently underway.

In Fig. 2, the main microstructural feature observed in both materials was the presence of a network of interconnected pores, as was reported by other authors [4, 5]. The porosity, rather complex, had the appearance of cavities with a high degree of interconnecting channels, the structure of which depends on the type of starch used in the processing. The sizes of these channels were also a function of the type of starch, according to their behavior in water at the consolidation temperature (mean size of swollen granules), among other factors. The material obtained from potato starch exhibited higher porosity associated mainly with large pores (100-μm mean equivalent diameter). Those materials obtained from cassava starch presented lower porosity with smaller pores (≈30 μm of mean equivalent diameter). Although less evident, the mean length of the channel of the C disks was greater than those of P disks.

Mechanical testing

Mechanical evaluation of sintered bodies was performed in diametral compression at different temperatures: *RT* [21], 800, 1000, and 1100 °C (heating rate of 10 °C/min). In this test, a uniaxial compressive load is applied diametrally on a disk until failure [12, 13, 22]. An INSTRON model 8501

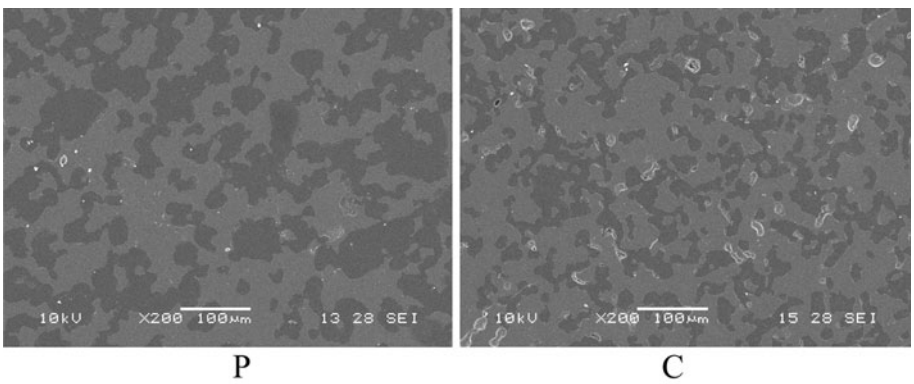

Fig. 2 SEM micrographs of sintered porous bodies

servohydraulic machine with a load cell of ±5kN of maximum load and a high stiffness load frame was used. The *RT* tests were performed using steel platens (R_c 65), and MoS_2 lubricant paste was applied between the specimen and the platens to reduce the effect of friction. Moreover, white and carbon papers were placed together between each platen and the specimen to distribute the load (padding material [22]). At high temperature, mullite/alumina rods were employed as load bearings, and no padding material was used, considering that the deformation at the load contact points is enough to distribute the load [12, 13, 22].

The tests were carried out in displacement control, using rates of 0.2 and 0.7 mm/min for room and high temperature tests, respectively (duration of tests ~1–1.5 min). A number of disks considered sufficient for statistical purposes were tested for each condition. The diameter of the tested disks (D) was four times greater than the thickness (t) to ensure a plane stress state ($t/D \leq 0.25$) [23]. This assumption is implicit in the theoretical treatment of the diametral compression loading case (Eq. 1) [22–24].

From the curves of experimental load versus displacement, the apparent ratio stress (σ) versus strain (ε) was obtained by calculus, using the following relationships [12, 13, 22–24]:

$$\sigma = \frac{2P}{Dt} \quad (1)$$

$$\varepsilon = \frac{d}{D} \quad (2)$$

where P is the load, D and t are the diameter and the thickness of the disk, respectively, and d is the actuator displacement. From σ versus ε curves, the following parameters were determined: mechanical strength (σ_F) using the first peak load, the apparent Young modulus (E_a) as the slope of the linear part of the curves, and the elastic limit (σ_Y) defined as the value of stress that corresponds to a deviation of deformation of 1% with respect to the linear behavior [12]. The ratio σ_Y/σ_F expressed as a percentage was considered indicative of the deviation from the linear behavior, i.e., an estimation of the degree of permanent deformation.

Fracture features of tested disks were analyzed by ocular inspection.

Results and discussion

Figure 3 shows the typical fracture patterns for each type of disks tested at different temperatures. The broken disks exhibited the following fracture patterns:

- Triple-cleft fracture (TCF): characterized by a central fissure that runs along the diametral axis of the load (diametral fracture, DF) together with secondary cracks that propagate parallel to the central fissure and break it in three (Fig. 3g) or more fragments (Fig. 3e, f) due to the additional failure of the internal fragments [22, 23, 25]. The shape of tongue and groove is characteristic of this type of fracture.
- Load Region Fracture (LRF): occurring in the region of contact between the disk and the compression platens, it consists of the presence of a clearly defined shear prism at generator, which in some cases culminates with small flakes of material becoming detached from the face of the cylinder adjacent to the platen contact (Fig. 3a). In extreme cases, a complete fragment of the disk can become separated (Fig. 3b, c). The fracture in the contact zone occurs due to compressive and shear stresses in this region despite being attenuated by the effects of load distribution. Some authors conclude that

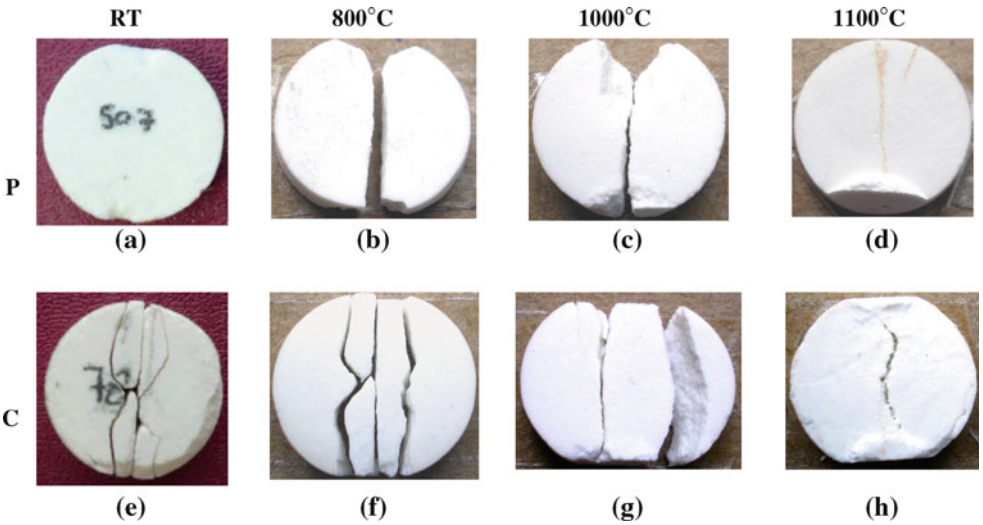

Fig. 3 Typical fracture patterns

this fracture type is invalid for the calculation of the mechanical strength using the Eq. 1 [22], although others consider that the test is still indicative of the bearing capacity of the material under the test conditions.

- Diametral Fracture (DF) plus LRF: even when diametral fracture (a unique central diametral fissure) did not occur alone, this type of failure was observed in combination with LRF.

At *RT*, disks obtained from potato starch (P) exhibited a higher tendency to LRF than C disks, which showed primarily TCF. At 800 °C, only TCFs were observed in C disks, and in P disks, DF plus LRF was also observed. At 1000 °C, the failure of disks was similar to that observed at 800 °C for both type of materials, and a flattening of the load contact region was also observed. This fact was more marked at 1100 °C, where the fracture of P and C disks was DF plus LRF associated with a large deformation at the load contact region, a well-developed shear prism, and a small portion of diametral fracture. These observations clearly show that a macroscopic permanent deformation (of a plastic nature) occurred in the specimens above 1000 °C, mainly at the load contact region.

Stress–strain curves for P and C disks as a function of testing temperature are shown in Fig. 4. Values of mechanical strength, apparent Young modulus, and σ_Y/σ_F ratio derived from curves are given in Table 1.

The initial region of stress–strain curves at *RT* (Fig. 4) showed a nonlinear segment that could be related to several factors: the specimen's arrangement in the load system, the load distribution in the load contact region, and/or elastic strains of the load system [12]. After this first region, an almost linear response was observed in C disks up to the sudden fall of the load due to the brittle manner in which the specimen failed, which was in agreement with fracture patterns (Fig. 3a, e). However, the registered curve for the disks obtained from potato starch showed a deviation from linearity before the specimen failure. This characteristic of the stress–strain curve for each type of disk was also expressed in the values of $\%\sigma_{y/}\sigma_F$ (Table 1): 93 and 70% for C and P disks, respectively.

Since no plastic deformation is likely to occur in the disks at *RT*, it was considered that the load distribution and the deviation from linearity in stress–strain curves were caused by microcracking. Crumbling of the material in the load contact region may also contribute to the load distribution.

During further thermal treatments, processing cracks in green bodies which were observed by SEM around the starch granules (Fig. 5) may close due to a chemical reaction between solid particles, propagate, or do not suffer any significant change. On the other hand, propagation of pre-existent cracks or the initiation of new fissures could also occur during cooling of the disks after the reaction-sintering treatment, since the system has multiple phases with different thermal expansion coefficients. Moreover, microcracks could be generated during the mechanical test.

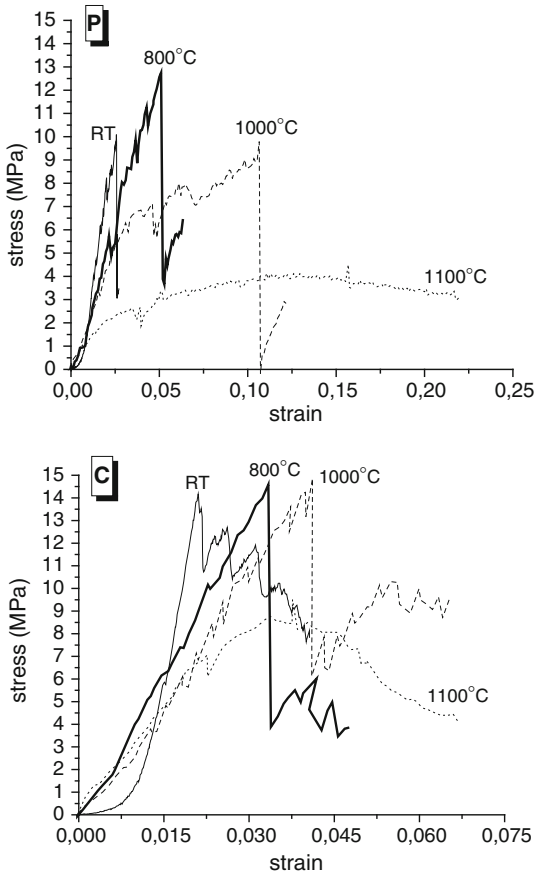

Fig. 4 Stress–strain curves as a function of testing temperature

Table 1 Values of mechanical parameters

	P		
	σ_F (MPa)	E_a (MPa)	$\%\sigma_{y/}\sigma_F$
RT	10.6 ± 1.5	580 ± 160	73 ± 21
800 °C	11.3 ± 1.8	454 ± 172	73 ± 6
1000 °C	8.2 ± 1.2	153 ± 88	68 ± 3
1100 °C	4.9 ± 1.1	183 ± 101	62 ± 20
	C		
	σ_F (MPa)	E_a (MPa)	$\%\sigma_{y/}\sigma_F$
RT	14.6 ± 2.6	1186 ± 345	93 ± 12
800 °C	14.0 ± 1.0	475 ± 20	98 ± 3
1000 °C	13.8 ± 1.3	442 ± 88	95 ± 7
1100 °C	7.1 ± 2.3	233 ± 135	77 ± 6

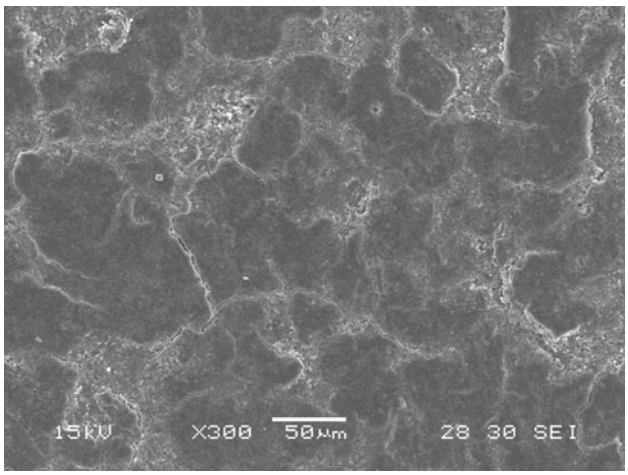

Fig. 5 SEM micrograph of a green body obtained using potato starch (processing cracks)

Owing to the presence of a little deviation from linearity in C disks tested at *RT*, the occurrence of microcracking cannot be ruled out. The difference with P disks could be attributed to the presence of higher amount of cracks in green bodies prepared using potato starch, as was inferred by SEM analysis. Moreover, the thermal process of starch removal in a matrix with weakly linked ceramic particles could be more disruptive in the case of potato starch due to the higher and more scattered sizes of granules. Another possibility could be that the higher volumes involved in these changes could increase the probability of initiating or propagating cracks. After the reaction-sintering treatment, the material obtained from potato starch would have more and/or larger cracks than C disks, which would favor microcracking.

For both types of disks tested at 800 °C, stress–strain curves were similar to those obtained at *RT*, which was also evident in $\%\sigma_y/\sigma_F$ values that remained constant. At 1000 °C, only stress–strain curves for P material differed in a higher degree with the previously analyzed curves, showing an earlier deviation from linearity (higher $\%\sigma_y/\sigma_F$ values). At 1100 °C, for P disks as much as C disks, a marked deviation from the linear behavior (significant decrease of $\%\sigma_y/\sigma_F$) was displayed, and the curves resembled that of a ductile material. In each case, the characteristics of the stress–strain curves were in agreement with the features of the fracture pattern. Above 1000 °C, in particular, a macroscopic permanent deformation (of plastic nature) was observed in the specimens, mainly at the load contact region.

At high temperatures, the deviation from linearity, more and more notable as temperature increased, was attributed to the presence of a silicate glassy phase that produced permanent plastic deformation. Based on Mg content in the system provided, in part, by impurities of raw materials, it is considered that this phase has a relatively high glassy transition temperature (T_g) at around 800 °C [26] and wets the crystalline phase grains (cordierite, spinel, and alumina). In the range of testing temperatures (800–1100 °C), especially at temperatures higher than 800 °C, this phase would be in a viscous state making it easier for the grains to slide due to a viscous flow mechanism when the load was applied. This process was considered mainly responsible for the behavior of both materials between 800 and 1100 °C.

The mechanical strength as well as the apparent Young's modulus of P disks evaluated at *RT* were lower than the values obtained for C disks at the same conditions (Table 1). In principle, both types of materials have the same cordierite-based matrix, and only differ in the porosity generated by the burning out of starches. This porosity was rather complex and hard to quantify by the most commonly used parameters (global porosity and pore sizes). First of all, considering the volume percentage of pores ($\%P_s$) as a measure of the global porosity, the higher value obtained for P disks would explain their lower values of σ_F and E_a. However, the incorporation of the effects of morphology and the mean size of pores is required to give a quantitative justification of the differences observed in the mechanical parameters of C and P disks, as was previously verified [21]. This requirement concerns above all the mechanical resistance values, which are determined not only by the amount of flaws but also by their size and sharpness.

Moreover, even though both types of disks have a cordierite-based ceramic matrix, it is possible that this matrix exhibits characteristics depending on the type of starches used in the consolidation step. These characteristics may affect the mechanical response of the porous material, such as the presence of different quantities and sizes of microcracks.

Plots of the mechanical strength and apparent Young's modulus values as a function of testing temperature are shown in Fig. 6.

The parameters σ_F and E_a varied by increasing the temperature although in general, the relative order between P and C disks followed the same tendency shown at *RT*. Even when the mechanical properties tended to decrease as temperature increased, mainly above 800 °C, the behavior of mechanical strength was different from that of the elastic modulus.

For C disks, the value of σ_F was almost constant up to 1100 °C (Fig. 6), where it showed a significant reduction. This decrease was attributed to the effect of the glassy phase softening that at this temperature was considered enough to favour the sliding of grains by viscous flow (plastic deformation) and, finally to grain separation (fracture). However, for P material, the decrease in

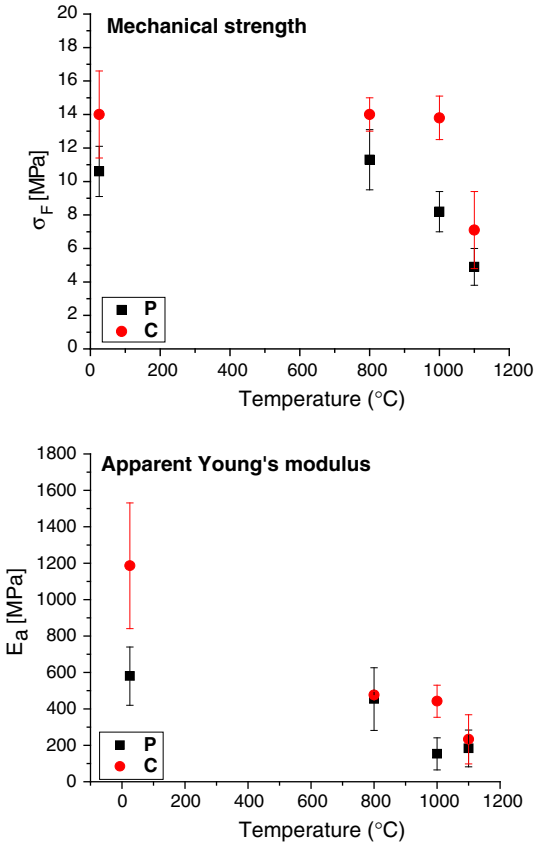

Fig. 6 Mechanical strength and apparent Young's modulus versus testing temperature

mechanical strength occurred at a lower temperature (1000 °C). This fact indicates that, at this temperature, the glassy phase was already acting negatively on the bearing capacity of the material. The fact that this effect did not become evident in C disks (keeping in mind that the glassy phase was very similar in composition and distribution in both materials) is explained by considering that the viscous phase could be occluded into pores, thus reducing their effect on the plastic deformation of the system. The smaller the pores, the higher the force retaining the viscous phase. In this way, the contribution of the viscous phase to deformation and fracture was also smaller. This was the case with C material, which exhibited smaller pores and narrower connection channels. At 1100 °C, the low viscosity of this phase prevailed over the blockage of the pores for both materials.

The behavior of apparent Young's modulus was different. In the case of C disks, a notable fall of the value at 800 °C with respect to that at *RT* was observed. This fact showed that some process increasing the capacity of deformation was activated at this temperature. On the other hand, this behavior was unexpected if the variation of the following properties between *RT* and 800 °C was considered: the mechanical strength of the C disks that was unchanged, and the value of E_a of P disks that only showed a small variation. The change of the glassy phase toward a viscous state had probably already occurred at 800 °C. The decrease of the Young's modulus value would confirm this fact. Nevertheless, it is also likely that the viscosity was still too high, and in this condition, it could favour the release of stress and/or blunting of crack (or microcracks) tip by plastic deformation, which shielded the applied stress and retained (or increasing slightly as observed in P disks) its value of mechanical strength.

The fact that no reduction in E_a was observed in P disks was accounted for considering that the same process discouraging the catastrophic crack propagation also decreased the microcracking (the main mechanism responsible for the stress–strain response).

At 1000 °C, a reduction of the parameter in P disks was observed while in C disks it remained practically constant. At this temperature, the viscous phase was more fluid, and it can displace toward pores where it was occluded, which reduced its effect on the deformation and loss of cohesion between grains. This effect prevailed in the case of C disks, which had smaller pores and more interconnections. For P disks where the blockage was lower due to the larger size of cavities, the higher fluidity of the viscous phase controlled the mechanical response.

At 1100 °C, the decrease of Young's modulus for C material has the same explanation as for the drop in mechanical strength. The slight increase of the value for P disks was attributed to the fact that due to the lower viscosity of the viscous phase at this temperature, this phase was completely distributed in the materials, thus achieving a positive effect (by blunting in the crack tip) over a high number of microcracks.

Differences in the composition or distribution of the glassy phase originating in the distinct characteristics of starches cannot be discarded; in fact, they could also explain the mechanical behavior of disks in the temperature range of testing. It is likely that the particular characteristics of starch granules (morphology and sizes) and the different generated porosity (morphology and size) affect the distribution of raw material particles in green bodies and the chemical reaction between these solid particles at a local level, thus generating differences in the composition or distribution of the glassy phase.

Conclusions

The mechanical behavior of cordierite-based porous bodies prepared by thermogelling of aqueous suspensions of a cordierite precursor mixture with potato or cassava starches was studied within a range of temperatures from *RT* to

1100 °C by using the diametral compression test. For both types of specimens, the response was rather different, with the disks prepared with potato starch exhibiting the lowest performance under load throughout the studied range of temperature. The materials showed a brittle behavior at room temperature, with an increase in the permanent deformation as temperature increased, until reaching a ductile response at the highest temperature (1100 °C). The differences observed in the variations of mechanical parameters with temperature between both types of materials were explained as being due to the effect of the porosity and glassy phase on the microcracking and the sliding of grains, which are considered the main mechanisms of permanent deformation and fracture of the specimens.

Acknowledgements The authors gratefully acknowledge Dr. M. I. Nieto and Ms. S. Benito (Instituto de Cerámica y Vidrio, CSIC, Madrid, España) for carrying out the measurements of pycnometric densities and particle size distributions of starches used in this study. This study was supported by CONICET (Argentina) under project (PIP 6255, 2006–2009).

References

1. Woyansky JS, Scott CE, Minnear WP (1992) Am Ceram Soc Bull 71(11):1674
2. International Outlook (1992) Am Ceram Soc Bull 71(12):1770
3. Studart AR, Gonzenbach UT, Tervoort E, Gauckler LJ (2006) J Am Ceram Soc 89(6):1771
4. Alves HM, Tari G, Fonseca AT, Ferreira JMF (1998) Mater Res Bull 33:1439
5. Lyckfeldt O, Ferreira JMF (1997) J Eur Ceram Soc 17:131
6. Pasbt W, Tynova E, Mikac J, Gregorova E, Havrda J (2002) J Mater Sci Lett 21:1101
7. Ratnayake WS, Jackson DS (2007) Carbohydr Polym 67:511
8. Almeida FA, Botelho EC, Melo FCL, Campos TMB, Thim GP (2009) J Eur Ceram Soc 29(9):1587
9. Minatti JL, Santana JGA, Fernandes RS, Campos E (2009) J Eur Ceram Soc 29(4):661
10. Barea R, Osendi M, Miranzo P (2005) J Am Ceram Soc 88:777
11. Subramaniam MA, Corbin DR, Chowdhry U (1993) Bull Mater Sci 16(6):665
12. Amorós JL, Cantavella V, Jarque JC, Felíu C (2008) J Eur Ceram Soc 28:701
13. Ozkan N, Briscoe BJ (1997) J Eur Ceram Soc 17:697
14. Tomba Martinez AG, Reboredo MM, Cavalieri AL (2007) J Mater Sci 42(13):5036. doi:10.1007/s10853-006-1403-y
15. Ovri JEO, Davies TJ (1987) Mater Sci Eng 98:109
16. Sandoval ML, Pucheu MA, Camerucci MA, Tomba M AG (2008) Evaluación mecánica de materiales porosos de cordierita obtenidos por consolidación directa con almidón. In: Anales 52° Congreso Brasilero de Cerámica, pp 1–12
17. Sandoval ML, Pucheu MA, Talou MH, AG TombaM, Camerucci MA (2009) J Eur Ceram Soc 29:3307
18. Talou MH, Villar M, Camerucci MA (2009) Ceram Int (in press)
19. Sandoval ML, Camerucci MA, Cavalieri AL, Scian AN (2007) Conformado por consolidación directa con almidón de precursores de materiales porosos de cordierita. In: Anales 51° Congreso Brasilero de Cerámica, pp 1–13
20. Smart RM, Glasser FP (1981) Ceram Int 7(3):90
21. Pucheu MA (2009) Evaluación mecánica de materiales cerámicos porosos mediante ensayos de compresión diametral. Tesis de grado, Universidad Nacional de Mar del Plata,
22. Darvell BW (1990) J Mater Sci 25:757
23. Fahad MK (1996) J Mater Sci 31:3723. doi:10.1007/BF00352786
24. Procopio AT, Zavaliangos A, Cunningham JC (2003) J Mater Sci 38:3629. doi:10.1023/A:1025681432260
25. Marion RH, Johnstone JK (1977) Am Ceram Bull 56:998
26. Camerucci MA, Al Cavalieri (2008) Ceram Int 34:1753